Eclipse Timing Variations of KIC 4150611 1.43d Eclipse Period and Characterisation of Potential Perturbing Object

James Phan[1] and Dr Ben Montet[1]

[1] *School of Physics, University of New South Wales, Australia*

Abstract: KIC 4150611 is a unique quintuple-star system encompassing 4 eclipsing binaries. We present our analysis on the eclipse timing variations of KIC 4150611 1.43d eclipse period and obtained characteristics of a potential perturbing object.

Keywords: Eclipse Timing Variations (ETVs), KIC 4150611, Eclipsing Binaries

1. INTRODUCTION

1.1 BACKGROUND

1.1.1 The Kepler Space Telescope

Space-borne telescopes have significantly improved today's understanding of stellar astrophysics. Their capacity to produce high-precision light curves has improved the analysis of eclipsing binaries and multi-eclipsing systems. The Kepler space telescope launched by NASA in 2009 is one such example. It was designed to determine the frequency of Earth-sized planets in and near the habitable zone of Sun-like stars (Borucki et al. 2010). However, due to its ability to precisely measure the dimming of the brightness of a star caused by another star, Kepler's initial release also detected 1879 eclipsing binaries (Prša et al. 2011). High-precision photometry of the eclipsing binaries enabled better analysis of their physical parameters and dynamics and also paved the way for the discovery and characterisation of potential exoplanets orbiting these systems.

1.1.2 KIC 4150611

KIC 4150611 is one of the brightest eclipsing binary systems observed by the Kepler space telescope. It is a rare multi-eclipsing quintuple system with four different periods of eclipses: 94.2, 8.65, 1.52, and 1.43d. Figure 1 represents the structure of the quintuple system as a set of 4 different eclipsing binaries, and the orbital periods between each component among other physical parameters are presented in Figure 2. The physical parameters showcased are derived in the latest analysis of KIC 4150611 by Hełminiak et al. (2017). More detailed parameters of the system are presented in the Multiple Star Catalog (Tokovinin 2018).

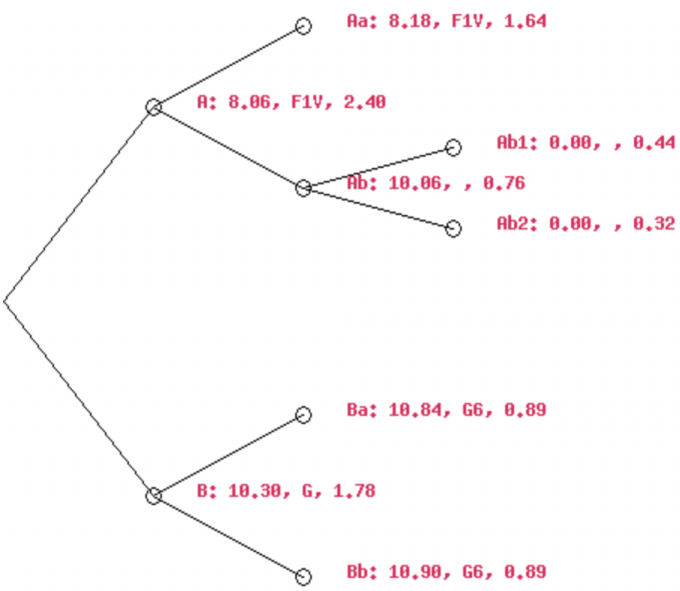

FIG. 1. Binary tree diagram from the Multiple Star Catalog (Tokovinin 2018) representing the structure of the KIC 4150611 system as 4 different eclipsing binaries. Legend: Component: Johnson's V Magnitude, Spectral Type, Mass.

Prm	Sec	Per	Sep	Vmag1	Vmag2	Mass1	Mass2
A	B	727.733y	1.137"	8.06	10.30	2.40	1.78
Aa	Ab	94.226d	4.733m	8.18	10.06	1.64	0.76
Ba	Bb	8.653d	0.872m	10.84	10.90	0.89	0.89
Ab1	Ab2	1.522d	0.206m	0.00	0.00	0.44	0.32

FIG. 2. The systems table from the Multiple Star Catalog (Tokovinin 2018) presents key physical parameters for each pair of eclipsing binary in KIC 4150611. Legend: Primary component, Secondary component, Orbital Period (days or years), Separation (milliarcseconds), Johnson's V Magnitude, and Masses (solar masses).

1.2 THEORY

1.2.1 Eclipsing Binaries

A binary star system is composed of two gravitationally bounded stars in orbit with one another. When binary systems orbit in the same plane containing a telescope's line of sight, it detects when the stars eclipse due to the relative decrease in brightness of the system. The light curve from Kepler shown in Figure 3 depicts dips representing this eclipsing phenomenon. Eclipsing binary systems have unique light curves that encode an abundance of information. Winn (2010) summarises the knowledge that has been gained through these eclipse observations.

1.2.2 Eclipse Timing Variations (ETVs)

A useful tool when observing eclipses/transits is the analysis of eclipse/transit timing variations (ETVs/TTVs) - precisely the main methodology applied in this research. Please note that the terms eclipses/transits and ETVs/TTVs will be used inter-

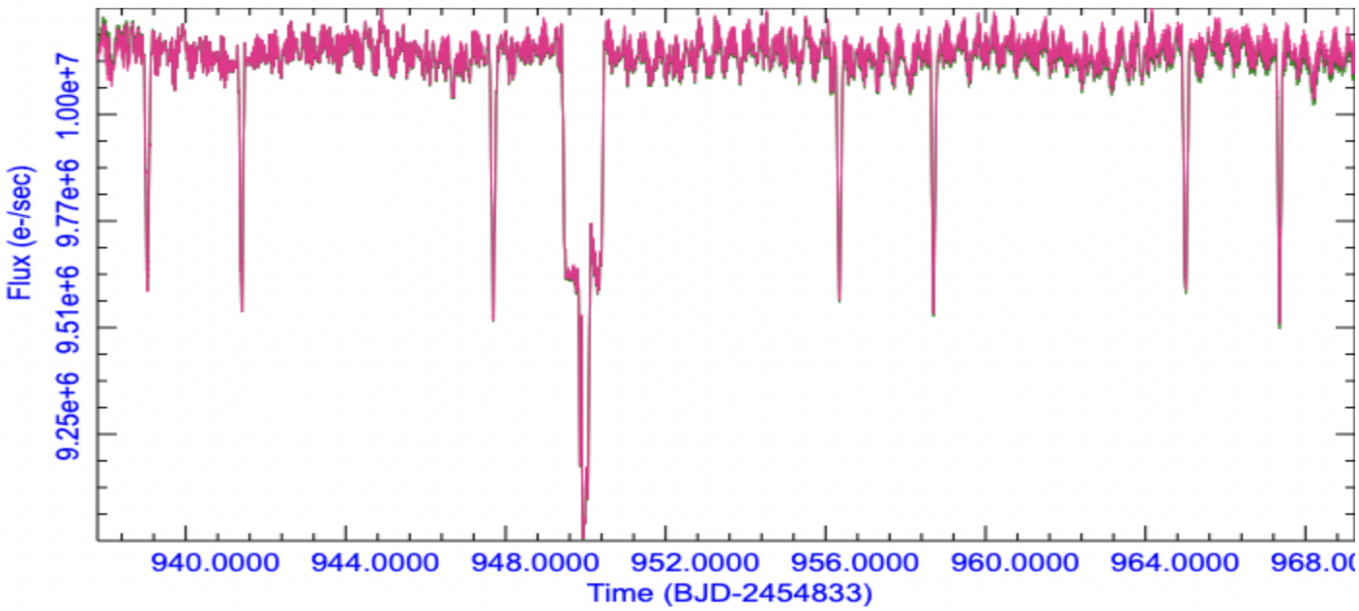

FIG. 3. The light curve of KIC 4150611 from quarter 10. The large drops in flux are caused by the eclipses within the system.

changeably as the concepts and techniques are identical.

In a perfect Keplerian orbit, the period of an orbiting object around its host star is constant and therefore we expect the eclipse times of eclipsing binaries to be periodic. Any ETVs would imply an additional factor perturbing the binary system, which is often the case due to the dynamic interactions with additional bodies. Planets orbiting binary star system exert a gravitational force that influences eclipse times, thus the analysis of ETVs offer an inferential way to detect exoplanets. Not only is it a neat tool for exoplanet detection, but the more impactful aspect of TTVs is also the characterisation of planetary systems in which multiple planets transit - one clear advantage of analysing ETVs is the ability to infer masses of perturbing objects directly in comparison to just eclipse photometry. The theory of TTVs is reviewed in Agol & Fabrycky (2018) with many citations to transit timing observations - examples include Ford et al. (2012), Steffen et al. (2012). The basics of TTVs are defined below.

The Keplerian constant-period model is used to predict eclipse times:

$$C = E \times P + T_0 \tag{1}$$

where C is the "calculated" eclipse time, E is the epoch (an integer eclipse number), P is the constant eclipse period and T_0 is the time of the first eclipse. "Observed" eclipse times are denoted by O, hence the perturbation due to another body can be represented in an $O-C$ plot - the difference between observed and calculated eclipse times. An $O-C$ plot from this research is shown in Figure 4. Values below the dotted line correspond to eclipses happening earlier than the Keplerian model, whereas values above mean eclipses occur later than the Keplerian model. Agol et al. (2005) defines TTVs as the accumulation of deviations from a constant transit period ($O-C$).

1.3 AIMS

1.3.1 The 1.43d Eclipse Period

Hełminiak et al. (2017) have not associated the 1.43d eclipse period to any component in KIC 4150611. Since the 1.43d eclipse period is prominent in all quarters of the Kepler mission, they expected the source to be close to the AB pair, and thus suspect the faint third star C captured in AO images - shown in Figure 5 - to be another eclipsing binary with a 1.43d orbital period. However at the time, Hełminiak et al. (2017) lacked the photometry to confirm this proposition.

We believe that the 1.43d eclipse period comes from the Ab1 and Ab2 binary. Based on the way the shape of the star changes on the detector, the data from Kepler suggests that the 1.43d signal comes from a very red object - Ab1 and Ab2 binary being the reddest stars in the system.

1.3.2 Aims

Our research initially attempts to confirm our belief of the origin of the 1.43d eclipse period. From there, our primary focus was analysing the ETVs in the 1.43d eclipse signal and modeling the ETVs in order to predict and characterise potential perturbing objects. This research is inspired by Hełminiak et al. (2017) as their analysis of KIC 4150611 hints at additional bodies in the system.

"*KIC 4150611 is one of the most interesting astrophysical discoveries of the Kepler mission, and we believe it deserves further attention.*" Hełminiak et al. (2017)

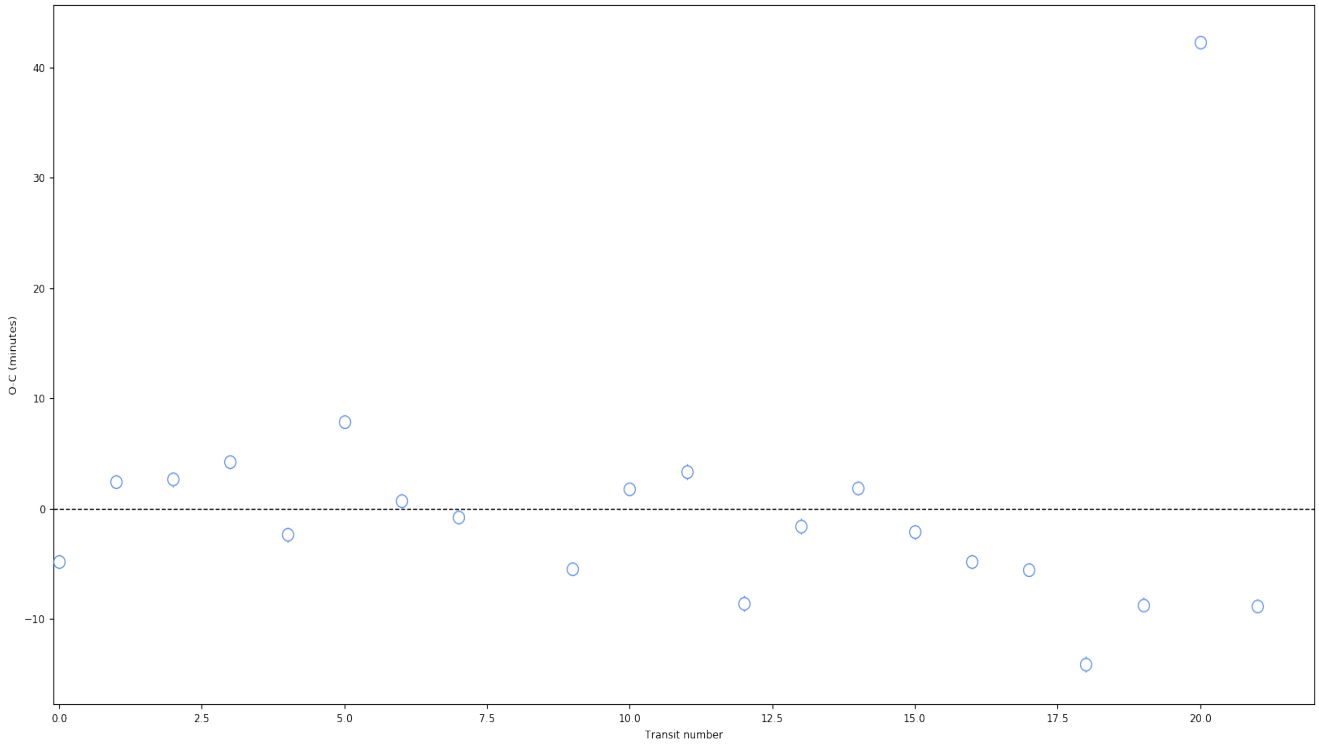

FIG. 4. An O-C plot from quarter 10. The Keplerian alternative model is represented by the dotted line which we expect each data point to lie on. Since the eclipse numbers are early/late, we infer that there is an additional body perturbing the Ab1/Ab2 component.

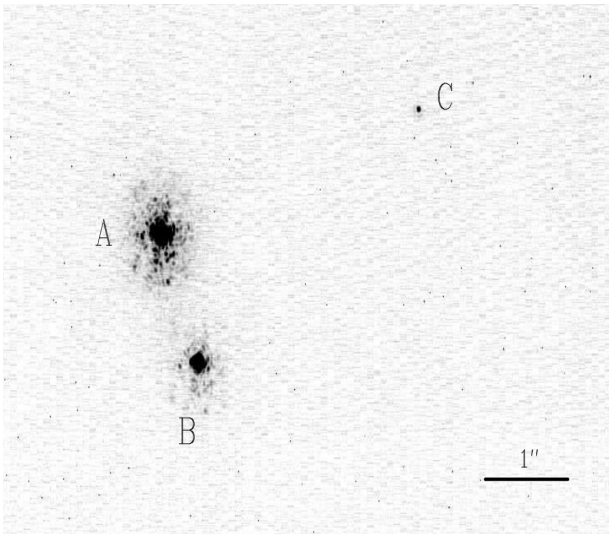

FIG. 5. Faint star C in the vicinity of the well-known visual binary ADS 12310 AB (KIC 4150611 system), which Hełminiak et al. (2017) suspects to be another eclipsing binary with orbital period 1.43d

2.DATA AND METHODOLOGY

2.1 DATA

2.1.1 Selection of Quarters

Our research uses the data collected from the Kepler mission available on Mikulski Archive for Space Telescopes (MAST). Despite having 18 quarters of data available for analysis, only quarters 7 to 15 (inclusive) were used for this research. This range was specifically chosen as the data was of short cadence type - a benefit of short cadence data is that light curves have better time sampling due to the shorter integration times which consequently allows for more precise calculation (Christiansen et al. 2010) - and allowed for effective comparison in contrast to the long cadence data used by Hełminiak et al. (2017) in their analysis of KIC 4150611. Even though only half of the available quarters were used, the time range from quarters 7 to 15 was sufficient in capturing any periodic trends of less than 2.5 years.

2.1.2 Filtering Kepler's Data

In order to focus on the specific 1.43d eclipsing signal from the Ab1/Ab2 binary pair, Kepler's data was processed to remove the pulsations from the A star and the deeper eclipses from other components following the methods of Hedges et al. (2021). Figure 6 shows the same light curve as Figure 3 after the filtering process. The periodic 1.43d eclipse is evidently more visible after the filtering process and allows for precise analysis of the Ab1/Ab2 targets.

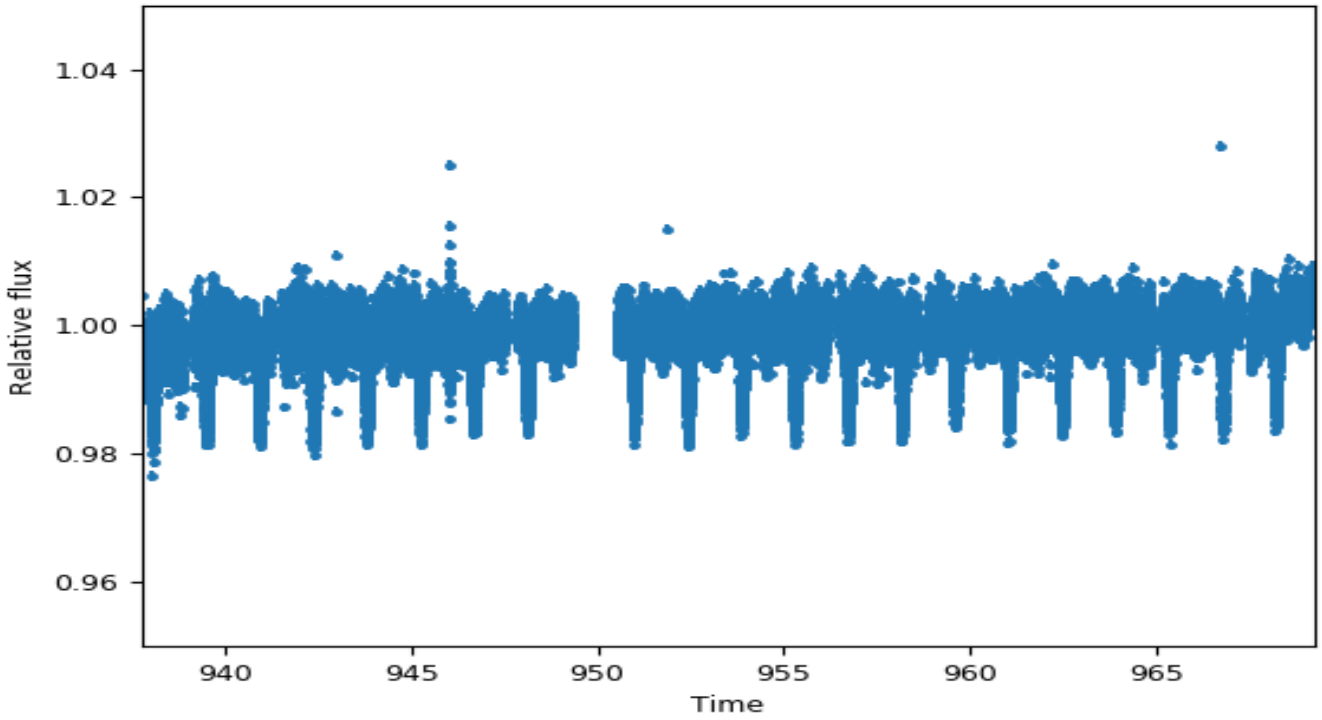

FIG. 6. The filtered light curve of KIC 4150611 from quarter 10 whereby the 1.43d eclipse signal is much more prominent.

2.2 METHODOLOGY

2.2.1 Fitting Light Curves with juliet

The filtered light curves are then fitted in order to determine the eclipse period and time of the initial eclipse - key parameters needed to estimate eclipse times using the Keplerian model (equation 1). To do this we relied on the python module juliet - a versatile modeling tool for transiting and non-transiting exoplanetary systems that can compute efficient fits to data coming from transit photometry and/or radial velocity (Espinoza et al. 2019). Note that juliet is a collective of different astronomy packages. Our research primarily uses batman (Kreidberg 2015) - a basic transit modeling and fitting package - and dynesty (Speagle 2020) - a dynamic nested sampling package for estimating Bayesian posteriors. These packages are valuable to our research as it allows for efficient computational analysis of the large dataset. The packages revolve around Bayesian Inference, in particular using nested sampling in order to make computational work feasible - a detailed look into nested sampling algorithms is reviewed in Buchner (2021).

Before juliet computes a fit on the light curve data, a set of prior information of parameters and corresponding distribution type and hyperparameters were given. The main aspect of this step is to give juliet a better idea of what the eclipse model might look like. The main contributing factor for the fit is feeding juliet initial guesses of the eclipse times - using the Keplerian model from equation 1 by setting $P = 1.43420486d$ (eclipse period found in Hełminiak et al. (2017)) and T_0 by rough inspection from the filtered light curve is a sufficient estimate.

The fitted light curve of Figure 6 is shown in Figure 7 where the black outline is the fitted eclipse model. There are often gaps within the Kepler data, most likely due to systematic errors or Kepler having to download the data back to Earth. As such it was an important detail not to supply an estimated eclipse time for juliet where there were missing data - if this were to happen, there would be irregularities in the eclipse model with significantly larger error in observed eclipse times (known based on experience). Apart from the fitted light curve, juliet also creates a data file - named posteriors.dat - of calculated physical parameters with a 68% confidence interval. This includes the fit's "observed" eclipse times O, needed to compute the ETVs against the fit's Keplerian model.

Note that each quarter is divided into 3 sections, and each section across quarters 7 to 15 was individually fitted. This is because the computational time for juliet to fit each section ranges from 5 hours to over 1 day, hence fitting for time ranges of over a third of a quarter is computationally demanding. UNSW's computer cluster Katana provided the computational resources for us to fit multiple sections at once (i.e a total of 27 fits were computed simultaneously in 27 separate job requests).

2.2.2 ETVs

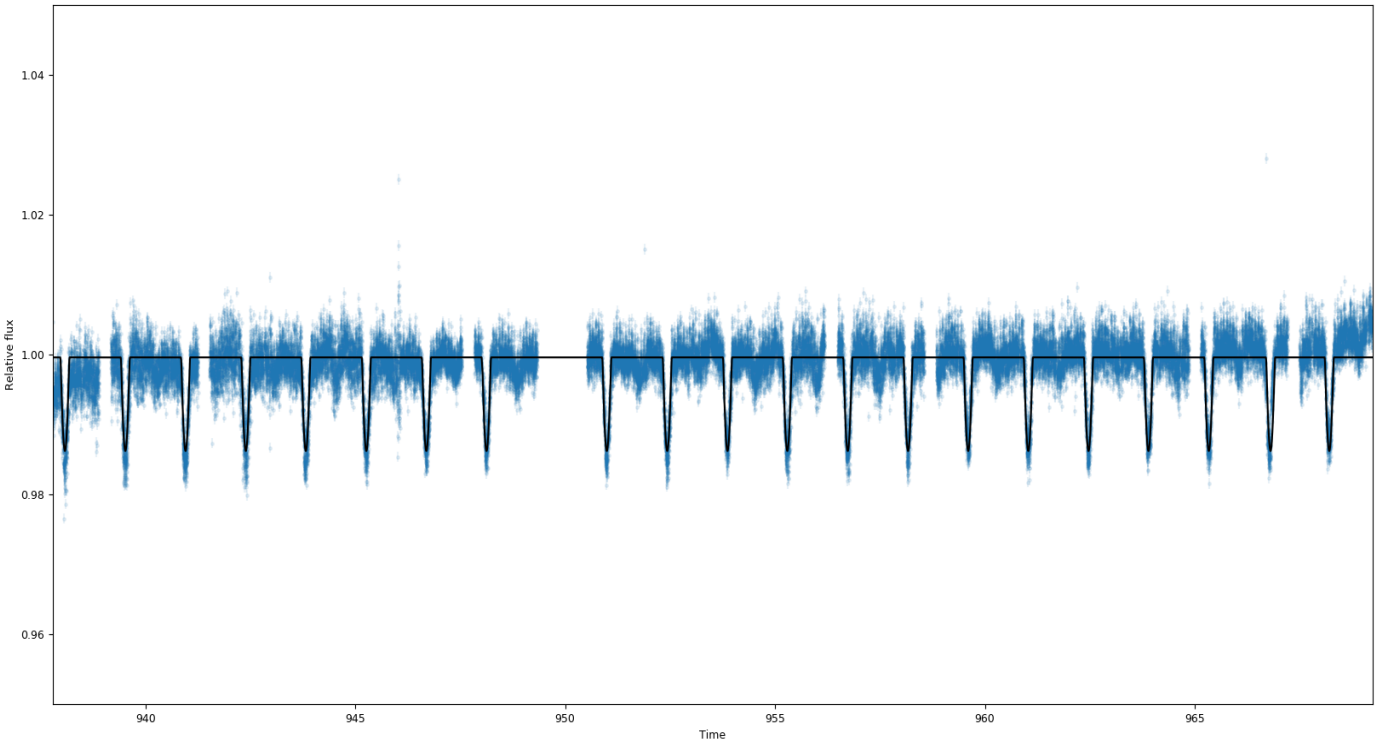

FIG. 7. The fitted light curve of KIC 4150611 from quarter 10 is outlined in black. Notice the shape of the dips are small and relatively even in size, confirming the origin of the 1.43d period was indeed from the Ab1/Ab2 component.

The ETVs for each section were plotted using the fitted observed eclipse times, eclipse period and initial eclipse time obtained from the respective posteriors.dat file. The observed eclipse times along with the 68% credibility band were subtracted from the calculated constant eclipse period model (equation 1) which were then scaled by a factor of 1440 to represent ETVs in minutes.

ETVs analysis of individual sections is ineffective in capturing longer periodic trends. In order to combat this, the ETVs from quarters 7 to 15 were then aggregated together, carefully accounting for discrepancies in fitted parameters. The new Keplerian model thus had a new eclipse period and initial eclipse time - the median of all eclipse period from the posterior data files was used along with the initial eclipse time of that specific posterior data file. Those two parameters is enough to compute an endless array of estimated eclipse times - with our particular range of interest being the start of quarter 7 to the end of quarter 15. Looping through all the posterior files, the observed eclipse times where subtracted from the new Keplerian model to give a stitched $O-C$ plot. The stitched $O-C$ plot shown in Figure 9 is then scaled to represent any ETVs signal in seconds with the x-axis now in unit days. Although ETVs signal in minutes is sufficient, the scaling into magnitudes of higher order allowed for easier computation in fitting a model through the ETVs.

The resulting $O-C$ plot is then fitted to our own defined function using the non-linear least squares method - as shown in Figure 10. Specifically, we used the optimize.curve_fit function in the scipy module, which when given our own defined function, set of data, and initial guesses of our function's coefficients, returns a function of best fit along with a covariance matrix that represents how well each coefficient represented the data. Providing a suitable function as well as initial coefficient guesses to fit the stitched $O-C$ plot was mostly by educated trial and error - we knew due to nature of the system that any trends in the data would be periodic and other known parameters such as the eclipse period of the A and B binary gave us a lead. A heat map of the log of the covariance matrix was closely used to examine how close or far the function of best fit was in representing the stitched ETVs signal. Furthermore, because the least squares method accounts for all data, it is heavily influenced by outliers, hence outliers were systematically removed in order to improve the accuracy of the curve of best fit.

3. RESULTS AND ANALYSIS

3.1 RESULTS

All results are saved here in the github repository: https://github.com/thejamesphan/KIC-4150611.git

The github repository includes filtered light curves

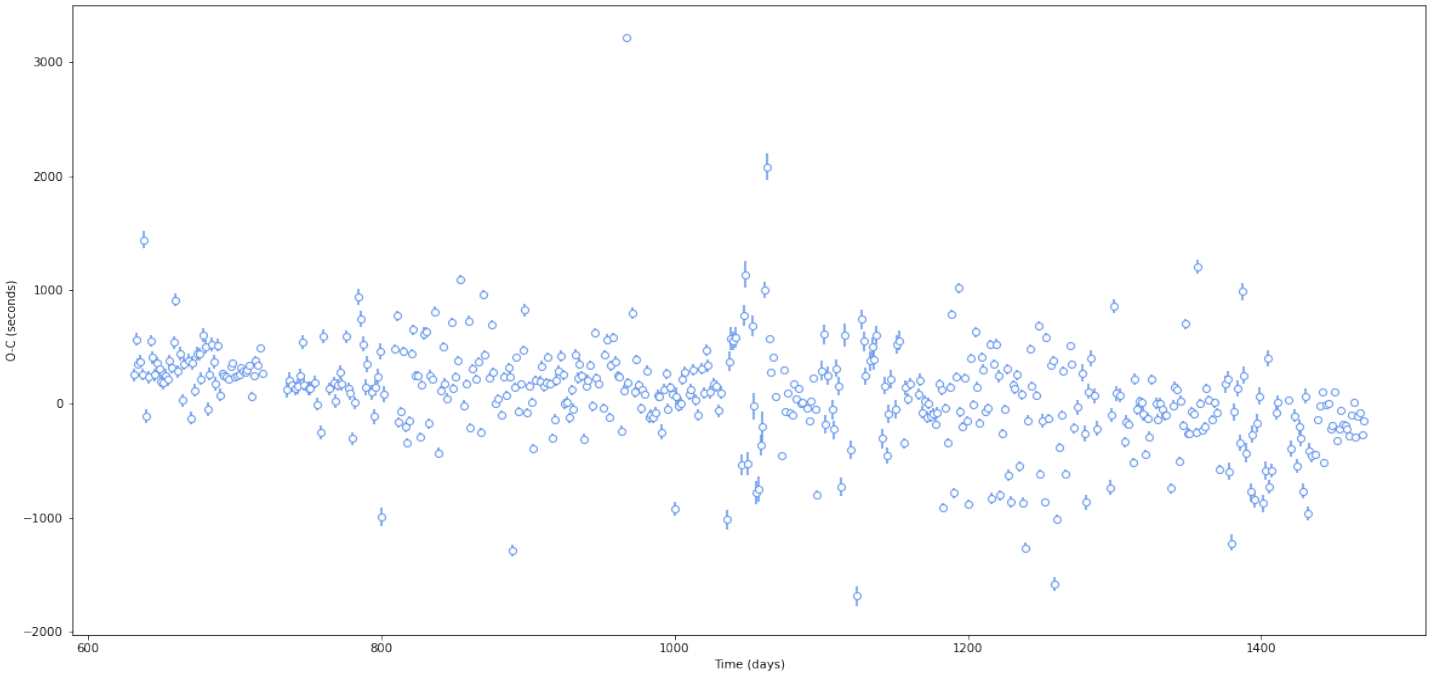

FIG. 8. The stitched O-C plot from quarters 7 to 15.

(e.g LC_q07_1), fitted light curves (e.g LC_FIT_q07_1), O-C plots (e.g OC_q07_1), and fitted physical parameters are saved in posteriors.dat file in corresponding quarter/section folders (e.g KIC4150611_TTV_q07_1)

3.2 ANALYSIS

3.2.1 The Eclipse Period of the Ab1/Ab2 binary pair

A satisfying confirmation that our filtered light curves did in fact target the M dwarfs (Ab1/Ab2) is through the shape of the eclipse model - (refer to Figure 7) since the shape of the dips were about the same size and the relative drop in fluxes was small, we can deduce that the source had to be small and relatively equal in size.

Across the 27 fitted light curves, the calculated eclipse period ranged from 1.4332876239d to 1.4346218712d. The 1.43420486d value obtained from the Hełminiak et al. (2017) falls well within our range, thus deeming our result accurate. Here we conclude the eclipse period of the Ab1 and Ab2 binary pair by taking the average of all calculated eclipse period with the uncertainty equal to the standard deviation. $(1.4341478767 \pm 0.0002814640)$d

3.2.2 ETVs

The stitched $O-C$ plot at first looked quite chaotic, however after several function fits were tried, a general trend of what was happening was deduced.

An initial function fit attempted was a pure sine function of the form:

$$a\sin(\frac{2\pi}{b}x + c) + d \tag{2}$$

where a is the amplitude of the ETVs signal, b is the period and c and d are translations and shifts of the sine function. The period oscillated towards an 85d signal which the heat map method suggests excellent relevancy in capturing the trend of the ETVs - we are happy to see this based on the similar result in Hełminiak et al. (2017) who confirmed strong significance of the 85d signal through an LS periodogram(Zechmeister & Kürster 2009) and frequency decomposer algorithm (Baluev 2013).

However, we did not settle with this function fit - here are the reasonings for our conclusive fit:

1. We already know that the M dwarfs binary itself orbited the F1V Star (A star), hence part of the function fit must account for this.

2. Since the obtained eclipse period of the Aa/Ab component is known to be 94.226 days, a sine fit of the 85d period would be inaccurate - we suspect the 85d signal is a combination of the Aa component along with at least another potential perturber, thus an additional sine function is required.

3. We noticed a clear long-term decline whereby the eclipse times near the start of quarter 7 were significantly later than the Keplerian model, and earlier towards the end of quarter 15. We accounted for this with an additional linear component - although it may even be a hint to another perturbing object with a much bigger orbital period.

The final function of best fit is as follows:

Parameter	Value
a	-3.79421388e+01
c	-3.43426136e+01
d	3.97865891e+01
e	9.89256371e-03
f	-3.42426640e+02
g	-5.45367755e-01
h	6.76520917e+02

FIG. 9. Values for the parameters in the optimal function fit to stitched O-C data.

$$a\sin(\frac{2\pi}{94.226}(x+c)) + d\sin(\frac{2\pi}{e}(x+f)) + gx + h \quad (3)$$

where the sum of the sine functions represents the influence from the F1V star and a potential perturber, the linear function represents a linear decreasing trend and translational and shift constants c,f,h. Note that since we knew the eclipse period of the F1V star, we fixed that specific coefficient 'b' as the least squares model was oscillating near that value anyway. Figure 9 shows the values of all coefficients, and Figure 10 is the resulting fitted curve against the stitched $O-C$ plot.

2 key results from the fitted function can be used to further characterise the perturber - namely the amplitude and period of the second sine function.

1. Orbital Period
The period of the second sine function is approximately 635 days, corresponding to the orbital period of the perturber.

2.Mass and Semi-Major Axis
The amplitude of the perturber's sine function corresponds to the light-time travel delay. In specific, the amplitude of 39.8 seconds meant that light from the Ab1/Ab2 component had to travel an additional 0.08 AU which corresponds to the semi-major axis. The mass and semi-major axis can be solved simultaneously through 2 equations - Kepler's Third Law and the mass to semi-major axis ratio between two objects. Note the beauty of these equations is that they do not assume whether the perturber is a star or an exoplanet.

$$\frac{M_p}{M_s} = \frac{a_s}{a_p} \quad (4)$$

$$P_p^2 = \frac{4\pi^2}{G(M_p + M_s)} a_s^3 \quad (5)$$

where P , M and a represent period,masses and semi-major axis, and the subscript p denotes the perturber. Since the perturber has an orbital period much greater than that of the F1V star around the Ab1/Ab2 component, subscript s denotes the entire A component. Inputting $M_A = 2.4, a_s = 0.08, P_p = 635/365$ (note units are in Earth days and AU), we obtained the mass of the perturber: $0.0974 M\odot$ and semi-major axis: 1.9628 AU. Figure 11 shows a summary of the potential perturber's parameters.

4.DISCUSSION

4.1 Short Cadence vs Long Cadence Choice

The outline of cadence type was briefly mentioned in section 2 - here we discuss the pros and cons. Overall the choice of cadence type did not lead to large discrepancies within results (for example the 1.43d eclipse period and 85 day ETV signal). Benefit of thus having chosen the short cadence route is to allow effective comparison with results of Hełminiak et al. (2017) and hence further improving the accuracy and validity of both research's results. Secondly, the shorter integration times of 1 minute in comparison to 30 minutes lead to a substantial increase of data to work with. Despite only using half the data available, 496 total eclipses from the Ab1/Ab2 binary were observed. A more extensive discussion on the impact of cadence choice is reviewed in Christiansen et al. (2010).

4.2 ETV and Multiple Star System

In comparison to the data, the fitted function has very low ETV amplitudes. This is mainly due to the notion of the fit obtained via the least squares method which is sensitive to all data present. Despite removing outliers to improve the fit, the resulting ETVs signal was low. This also suggest the perturber may not be close to resonance to the system - detailed relation to TTVs amplitude and resonance is discussed at lengths in Agol & Fabrycky (2018).

On a more interesting note, the field of multiple star systems is very fascinating but not well understood - possibly because the maths gets complicated with higher order hierarchies. There are many open questions in regard to their formation and dynamic interactions. KIC 4150611 is a quintuple system with many hidden dynamical interactions behind the scenes - all of which cannot be easily understood from ETVs alone. A better understanding of multiple star system dynamics will in turn lead to better ETV analysis.

4.3 Uncertainty in Perturber's Parameters

The characteristic results are very much plausible, but unfortunately due to the scope of this research, the uncertainty of the given values could not be determined. In order to give absolute parameters of the perturber, further detailed analysis is required in all aspects of this research. The timing precision in the individual eclipse times needs to be considered as there is photometric uncertainty during ingress and egress of a transit (Agol & Fabrycky 2018). Furthermore, investigating the individual o-c data and determining whether or not we believe those ETVs will conclude in a more accurate model of the system.

4.4 Improvements and Future Prospect

An extension of this research in order to build on and/or improve includes:

1. Extending the input dataset to incorporate all

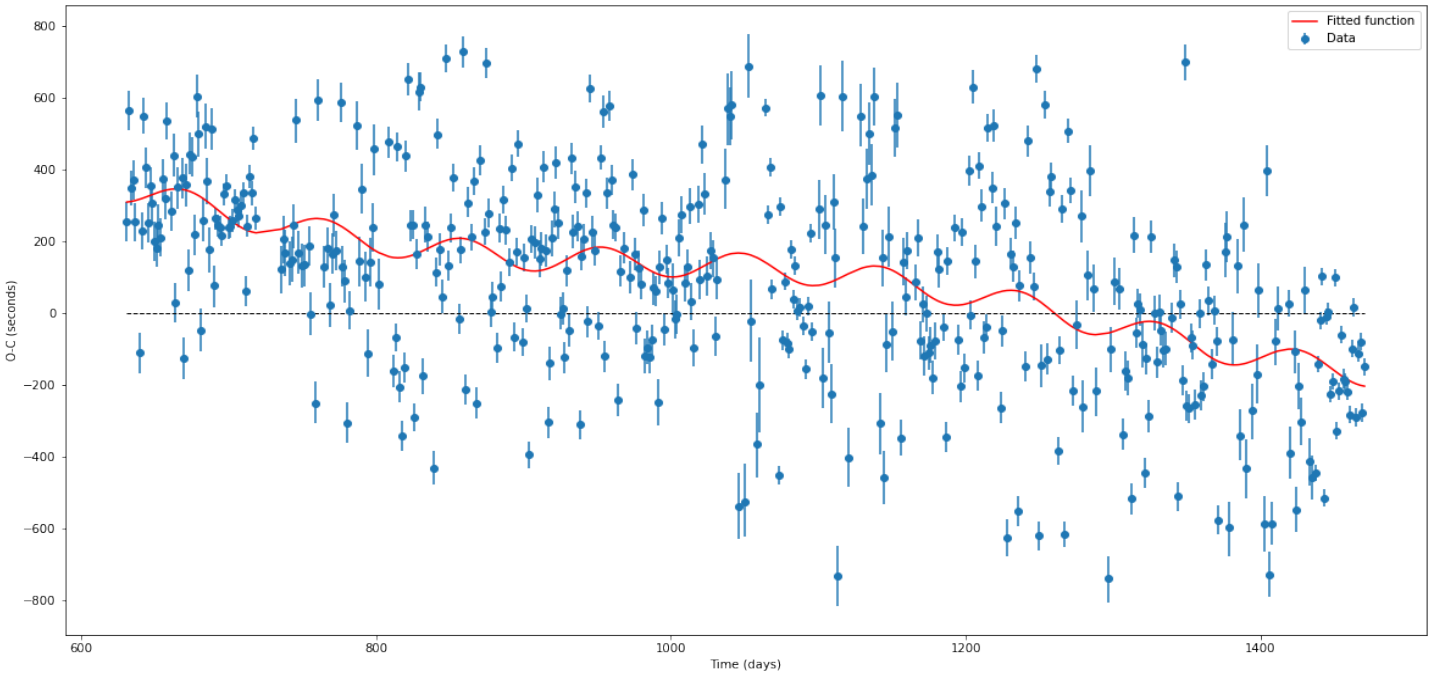

FIG. 10. The fitted function against the stitched O-C plot. It is the sum of two sine functions corresponding to the perturbation influence of the F1V Star and a potential perturber.

Parameter	Value
Period	635.14226356 d
Mass	0.0974892 $M\odot$
Semi-major Axis	1.96284829359 AU

FIG. 11. Characterisation of the Potential Perturbing Object

quarters. This will help improve the current model of the ETVs, confirming this research's presented findings and capturing even larger perturbation influences of larger orbital scales. The linear component of the fitted function already hints at an additional body influencing at a bigger timescale.

2. The resulting ETVs data is extremely valuable in understanding multi-body systems and gives means to the exploration of the dynamics in multi-star systems. An extension of this research hence would be to attempt to model and simulate the dynamical interactions within KIC 4150611 and how that would affect the lightcurves and ETVS.

3. Improving the accuracy of this research by considering uncertainty in eclipse times. In particular, more consideration towards timing precision and fitting for perturbations in each individual eclipse times directly (i.e using Bayesian Inference to fit for eclipse timing perturbation).

CONCLUSION

Overall, the research aims were successfully met. Through the analysis of Eclipse Timing Variations of KIC 4150611 1.43d Eclipse Period, a potential perturber was inferred and its characteristics were calculated. Further extensions of this research is presented. We too, like the Hełminiak et al. (2017), believe KIC 4150611 is a very interesting system worthy of further analysis.

REFERENCES

Agol, E., & Fabrycky, D. C. 2018, in Handbook of Exoplanets, ed. H. J. Deeg & J. A. Belmonte, 7, doi: 10.1007/978-3-319-55333-7$_7$

Agol, E., Steffen, J., Sari, R., & Clarkson, W. 2005, , 359, 567, doi: 10.1111/j.1365-2966.2005.08922.x

Baluev, R. V. 2013, , 436, 807, doi: 10.1093/mnras/stt1617

Borucki, W. J., Koch, D., Basri, G., et al. 2010, Science, 327, 977, doi: 10.1126/science.1185402

Buchner, J. 2021, arXiv e-prints, arXiv:2101.09675. https://arxiv.org/abs/2101.09675

Christiansen, J., Jenkins, J. M., Caldwell, D. A., et al. 2010, in AAS/Division for Planetary Sciences Meeting Abstracts, Vol. 42, AAS/Division for Planetary Sciences Meeting Abstracts #42, 59.03

Espinoza, N., Kossakowski, D., & Brahm, R. 2019, , 490, 2262, doi: 10.1093/mnras/stz2688

Ford, E. B., Fabrycky, D. C., Steffen, J. H., et al. 2012, Astrophys. J., 750, 113, doi: 10.1088/0004-637X/750/2/113

Hedges, C., Luger, R., Dotson, J., Foreman-Mackey, D., & Barentsen, G. 2021, , 161, 95, doi: 10.3847/1538-3881/abd31c

Hełminiak, K. G., Ukita, N., Kambe, E., et al. 2017, , 602, A30, doi: 10.1051/0004-6361/201630379

Kreidberg, L. 2015, Publications of the Astronomical Society of the Pacific, 127, 1161, doi: 10.1086/683602

Prša, A., Batalha, N., Slawson, R. W., et al. 2011, , 141, 83, doi: 10.1088/0004-6256/141/3/83

Speagle, J. S. 2020, , 493, 3132, doi: 10.1093/mnras/staa278

Steffen, J. H., Fabrycky, D. C., Ford, E. B., et al. 2012, , 421, 2342, doi: 10.1111/j.1365-2966.2012.20467.x

Tokovinin, A. 2018, VizieR Online Data Catalog, J/ApJS/235/6
Winn, J. N. 2010, arXiv e-prints, arXiv:1001.2010. https://arxiv.org/abs/1001.2010
Zechmeister, M., & Kürster, M. 2009, , 496, 577, doi: 10.1051/0004-6361:200811296